

September 11, 2015

## Charm and bottom quark masses on the lattice

ANDREW T. LYTLE

*SUPA, School of Physics and Astronomy  
University of Glasgow, Glasgow, G12 8QQ, UK*

Lattice determinations of quark mass have made significant progress in the last few years. I will review recent advances in calculations of charm and bottom mass, which are near to achieving percent-level precision and with fully controlled systematics. Precise knowledge of these parameters is of particular interest for precision Higgs studies at future accelerators.

PRESENTED AT

The 7th International Workshop on Charm Physics  
(CHARM 2015)  
Detroit, MI, 18-22 May, 2015

# 1 Introduction

Quark masses are fundamental parameters entering into the definition of the Standard Model. Within the Standard Model picture, quark masses arise from Yukawa interactions with the Higgs field, and direct measurements of the Higgs couplings at the LHC are consistent with Standard Model predictions. High-precision studies at future accelerators such as the ILC will measure couplings at the per mil level [1]. In order to test the SM at this level, and to constrain and potentially discriminate between models of new physics detectable at this level, it is imperative to determine the quark masses to a corresponding level of precision.

In recent years, considerable progress has been made in lattice calculations of quark masses, with groups now quoting charm and bottom mass values at around the percent or few-percent level. This is due to increasingly realistic simulations, and new techniques. State-of-the-art simulations include dynamical  $u, d, s$ , and frequently  $c$  quarks, with pion masses reaching their physical values, and typically at several lattice spacings. This increased realism translates into increasingly accurate results, and with fewer systematic errors. In order to reliably determine quark masses at the sub-percent level, it is important to have a variety of calculational techniques/strategies available, along with independent determinations from different groups.

The outline of the rest of this article is as follows: Sec. 2 briefly discusses quark mass parameters in a general context, and how they are determined in lattice QCD simulations. In Sec. 3 I will discuss recent progress in the charm mass determinations, focusing on a promising method using current-current correlators. Sec. 4 will look at strategies and results for bottom mass determinations, and Sec. 5 discusses the important role played by mass ratios. Sec. 6 presents a summary and discusses future prospects for these calculations.

## 2 Quark mass and LQCD

Quark masses are scheme and scale dependent quantities and can be viewed as input parameters that, along with  $\alpha_s$ , specify QCD at the Lagrangian level. These parameters must ultimately be determined from experiment, but because quarks are confined into hadrons the connection is necessarily indirect. In the absence of lattice simulations, one must focus on experimentally measureable observables which are 1) sensitive to quark masses and 2) can be reliably computed in perturbation theory. One set of observables satisfying these criteria are derived from the R-ratio. Much effort has gone into calculation of the relevant perturbation series, which are now known to N<sup>3</sup>LO [2, 3, 4]. As will be discussed in Sec. 3.1, one promising way to calculate  $m_q$  for heavy quarks via lattice simulations uses the same perturbative calculations, but substitutes experimental data with data from LQCD simulations.

Lattice QCD simulations are well suited for mass determinations, since the mass parameters are simulation inputs controlled by the “experimenter”. By changing the input masses, one can directly measure the resultant change in physical observables. In a standard LQCD simulation, one tunes the input masses in order to reproduce the masses of some low-lying hadrons – one for each quark in the theory. In this way one obtains (typically very precise) bare quark masses, but in the particular lattice regularization one happens to be using. In order to make contact with a continuum-regularized determination such as the  $\overline{\text{MS}}$  scheme, one needs an additional calculation of the lattice to  $\overline{\text{MS}}$  matching factor. This can be found using lattice perturbation theory or via non-perturbative renormalization (NPR) techniques. The ratios of bare quark masses in a given regularization are however immediately useful, as they are equal to renormalized mass ratios (up to lattice artifacts).

### 3 Charm quark mass

#### 3.1 Current-current correlator method.

The current-current correlator method uses moments of Euclidean-time twopoint functions,

$$G(t) = a^6 \sum_{\mathbf{x}} (am_{0h})^2 \langle J_5(t, \mathbf{x}) J_5(0, 0) \rangle. \quad (1)$$

Here  $J_5 \equiv \bar{\psi}_h \gamma_5 \psi_h$  and  $am_{0h}$  is the bare quark mass parameter in lattice units. In formalisms with sufficient chiral symmetry, the current  $J_5$  is absolutely normalized. The correlator  $G(t)$  is UV finite, so that

$$G(t)_{\text{cont}} = G(t)_{\text{latt}} + \mathcal{O}(a^2) \quad (t \neq 0). \quad (2)$$

The correlators  $G(t)_{\text{latt}}$  are the same ones used to compute pseudoscalar masses and decay constants, in which case it is the large- $t$  exponential tail of the correlator that is of interest. For the mass calculation it is the small- $t$  short distance behavior that is extracted via time-moments of  $G(t)$ , defined as:

$$G_{n,\text{latt}} = \sum_{t=0}^T (t/a)^n G(t)_{\text{latt}}. \quad (3)$$

The time-moments  $G_n$  have also been computed to N<sup>3</sup>LO in perturbation theory [2, 3, 4]. For  $n \geq 4$ ,

$$G_{n,\text{pert}} = \frac{g_n(\alpha_{\overline{\text{MS}}}, \mu)}{(am_h(\mu))^{n-4}}. \quad (4)$$

Here  $m_h(\mu)$  is the  $\overline{\text{MS}}$  quark mass at the scale  $\mu$ . The basic strategy to extract the quark mass is to compare  $G_{n,\text{cont}}$ , the continuum extrapolated  $G_{n,\text{latt}}$  values, with the

perturbative expressions  $G_{n,\text{pert}}$  in Eq. (4) (evaluated at a scale  $\mu \sim m_h$ ), and from these determine best-fit values for  $\alpha_{\overline{\text{MS}}}(\mu)$  and  $m_h(\mu)$ . For example, computing the continuum limit of  $G_{4,\text{latt}}$  with physically tuned input charm masses  $m_{0c}$ , one can obtain  $\alpha_{\overline{\text{MS}}}(m_c)$ , and then use this value in  $G_6$  to obtain  $m_c(m_c)$ .

The HPQCD collaboration carried out an analysis in [5] using reduced moments,  $R_n$ , which are simply related to the time-moments as

$$R_4 = G_4/G_4^{(0)} \quad (5)$$

$$R_n = \frac{1}{m_{0c}} (G_n/G_n^{(0)})^{1/(n-4)} \quad (n \geq 6). \quad (6)$$

where  $G_n^{(0)}$  are the tree-level results for the moments. Dividing by  $G_n^{(0)}$  has the advantage of reducing lattice-spacing effects. In continuum perturbation theory,

$$R_4 = r_4(\alpha_{\overline{\text{MS}}}, \mu) \quad (7)$$

$$R_n = \frac{1}{m_c(\mu)} r_n(\alpha_{\overline{\text{MS}}}, \mu) \quad (n \geq 6). \quad (8)$$

Here  $r_n$  are the perturbative expressions given by appropriate powers of  $g_n/g_n^{(0)}$ , with  $g_n^{(0)}$  the lowest order perturbative result. For a given  $m_{0h}$  one computes the values of  $R_n$  from Eq. (6) and gets an estimate of  $m_c(3m_h) = R_n/r_n(3m_h)$ , via Eq. (8) (the scale  $\mu$  was taken to be  $3m_h$ ). In this way the scale dependence of  $m_c^{\overline{\text{MS}}}(\mu)$  is determined.

The running of  $m_c(\mu)$  was calculated this way in [5] using  $n_f = 2 + 1 + 1$  HISQ ensembles. The  $n = 4, 6, 8, 10$  moments were computed using three different lattice spacings  $a \approx 0.12, 0.09, 0.06$  fm and for seven input masses from  $m_h = m_c - 0.7m_b$ . The extractions of  $m_c(3m_h)$  from each of these data points are shown in Fig. 1 (left), along with the perturbative running. Fig. 1 (right) shows the corresponding estimate of  $\alpha_s$  extracted from this data, ran to  $M_Z$  and compared with results based on other experimental inputs.

Estimates of  $m_c(\mu)$  from time-moments are subject to a number of systematic uncertainties. The truncation of perturbation theory of course limits the precision. Fortunately the expansions of  $r_n = 1 + \sum_j \alpha^j r_{nj}$  are known for  $j = 1, 2, 3$  and  $n \leq 10$ . The lattice moments are sensitive to condensate terms not captured in the perturbative expansions. These effects are suppressed like  $(\Lambda_{\text{QCD}}/2m_h)^4$ , but they also grow with  $n$ . The lattice data also has cut-off effects, which grow like  $\alpha_s(am_h)^2$  and decrease with increasing  $n$ ; these trends are visible in Fig. 1.

Fitting the moments data for  $n = 4, 6, 8, 10$  to Eqs. (7) and (8), HPQCD find

$$m_c^{\overline{\text{MS}}}(3 \text{ GeV}, n_f = 4) = 0.9851(63) \text{ GeV} \quad (9)$$

$$\alpha_s^{\overline{\text{MS}}}(3 \text{ GeV}, n_f = 4) = 0.2545(37). \quad (10)$$

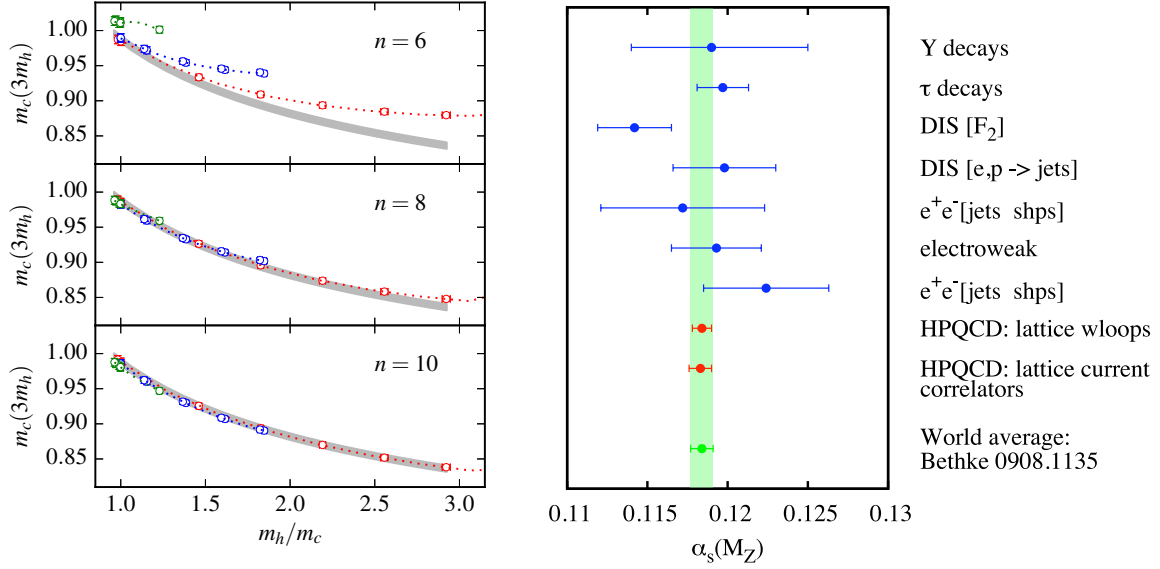


Figure 1: (Left) Data from [5] showing  $m_c^{\overline{\text{MS}}}(\mu = 3m_h)$  extracted from lattice data and perturbation theory for moments  $n = 6, 8, 10$  using Eq. (8). The green/blue/red data points correspond to lattice spacings of 0.12/0.09/0.06 fm. The gray band shows the evolution of the best-fit value for  $m_c$  using perturbation theory. (Right) Value of  $\alpha_s^{\overline{\text{MS}}}(M_Z)$  from [5] compared with determinations based on various experimental inputs and a world average.

These are compatible with earlier  $n_f = 2 + 1$  results [6]. The compatibility of  $n + f = 2 + 1$  and  $n_f = 2 + 1 + 1$  results suggests that the effect of charm quarks in the sea can be treated perturbatively, to this level of precision.

The JLQCD collaboration has recently utilized the current-current correlator method with  $n_f = 2 + 1$  domain-wall fermions to determine  $m_c$  and  $\alpha_s$  [7]. Their calculation uses three lattices spacings  $a \approx 0.08, 0.055, 0.044$  fm, and focuses on  $R_6, R_8$ , and  $R_{10}$ , from which they find

$$m_c^{\overline{\text{MS}}}(3 \text{ GeV}, n_f = 3) = 0.9936(91) \text{ GeV} \quad (11)$$

$$\alpha_s^{\overline{\text{MS}}}(3 \text{ GeV}, n_f = 3) = 0.2526(92). \quad (12)$$

### 3.2 Comparison of results

In [8] the ETMC collaboration use lattice RI/MOM techniques to determine a mass renormalization factor  $Z_m^{\text{RI}}(\mu, 1/a)$  connecting the bare mass to the RI-scheme mass,  $m_c^{\text{RI}}(\mu) = Z_m^{\text{RI}}(\mu, 1/a) m_{c0}$ , which is converted to the  $\overline{\text{MS}}$  scheme using continuum perturbation theory. Unlike the current-current correlator method, which uses a heavy input mass to set the scale  $\mu$ , the RI/MOM calculation is extrapolated to

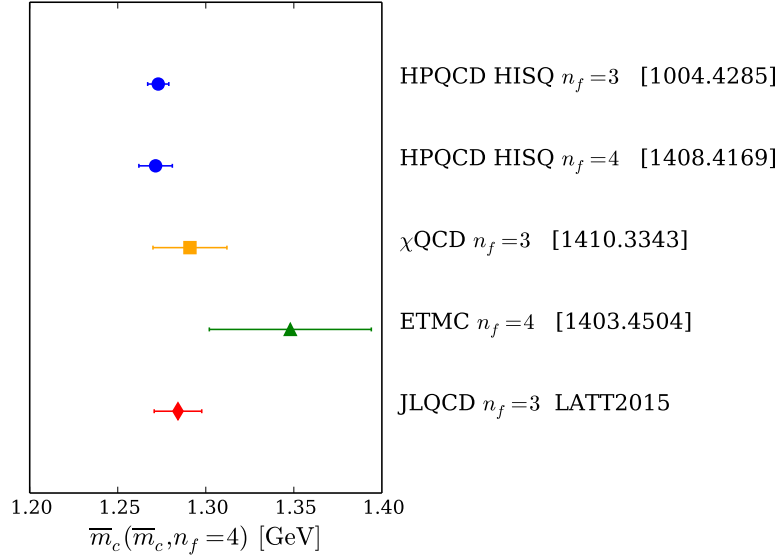


Figure 2: Comparison plot for determinations of  $m_c^{\overline{\text{MS}}}(m_c^{\overline{\text{MS}}}, n_f = 4)$ , computed from  $n_f = 2 + 1$  and  $n_f = 2 + 1 + 1$  simulations.

the chiral limit, and ETMC have generated mass degenerate  $n_f = 4$  ensembles for this purpose. The  $\chi$ QCD collaboration have also used RI/MOM methods for their  $n_f = 2 + 1$  determination [9, 10].

A comparison of recent lattice results for  $m_c^{\overline{\text{MS}}}$  is shown in Fig. 2.

## 4 Bottom mass

It is challenging to directly simulate the  $b$  mass in relativistic lattice simulations, since one would like  $am_{b0} \ll 1$  to keep discretization effects under control. Instead effective theories may be employed such as non-relativistic QCD (NRQCD) or heavy-quark effective theory (HQET). It has recently become possible with improved relativistic actions to approach the  $b$  mass, making extrapolation methods viable.

### 4.1 NRQCD approach

The NRQCD Hamiltonian is written as an expansion in  $v^2$ , where  $v$  is a typical velocity of a  $b$  quark in the system of interest. For example,  $v^2 \sim 0.1$  in the  $\Upsilon$  meson. NRQCD calculations should be carried out with  $am_{b0} > 1$ . This has the advantage that the  $b$  can be simulated using relatively coarse lattices, on the other hand it is less straightforward to extract continuum physics as compared to relativistic calculations.

The NRQCD current-correlator approach [11] is similar to the relativistic approach described in Sec. 3.1. One studies the time-moments of Euclidean-time two-point correlators. Unlike in the relativistic case, here the currents need to be normalized,

$$J_\mu^{\text{NRQCD}} = Z_V J_\mu^{\text{cont}}. \quad (13)$$

Then the time moments are related to continuum perturbation theory,

$$G_n^{\text{NRQCD}} = Z_V^2 \frac{g_n(\alpha_{\overline{\text{MS}}}, \mu)}{(am_b(\mu))^{n-2}}. \quad (14)$$

Constructing ratios of successive moments, the factors of  $Z_V$  can be canceled. Because the continuum limit cannot be approached directly one instead studies  $m_b$  as a function of the moment number. Compared to the charm case, condensate contributions which grow with moment number are more suppressed at the heavier quark mass. A “plateau” in  $m_b$  as a function of moment number implies that  $n$  is sufficiently large for discretization effects to be small. Such a plateau from [11] is shown in Fig. 3 (left).

Results at three lattice spacings and with two different light-quark masses for  $n = 18$  are shown in Fig. 3 (right). A fit to this data, including systematic errors, and perturbatively evolved to  $m_b$  gives

$$m_b^{\overline{\text{MS}}}(m_b^{\overline{\text{MS}}}, n_f = 5) = 4.196(23) \text{ GeV}. \quad (15)$$

This result is compared with others in Fig. 4. It is significant that the values in the figure are calculated using a range of techniques. In [6] results are extrapolated to  $m_b$  from below, using a relativistic action as described in Sec. 3.1. This calculation is based on a different range of moment numbers, and uses a different action than [11]. The work of [12] uses the binding energy of  $\Upsilon$  and  $B_s$  mesons, computed using NRQCD and lattice perturbation theory, to determine the heavy quark pole mass, which is then converted to the  $\overline{\text{MS}}$  mass with continuum perturbation theory.

## 4.2 Ratio method

The ETMC collaboration have used the *ratio method* [13] to extrapolate relativistic  $n_f = 2 + 1 + 1$  simulation results around the charm mass to the bottom mass [14]. The method is based on the expectation from HQET that

$$\lim_{m_h^{\text{pole}} \rightarrow \infty} \frac{M_{hl}}{m_h^{\text{pole}}} = \text{constant}, \quad (16)$$

where  $M_{hl}$  is the mass of a heavy-light meson and  $m_h^{\text{pole}}$  is the heavy quark pole mass.

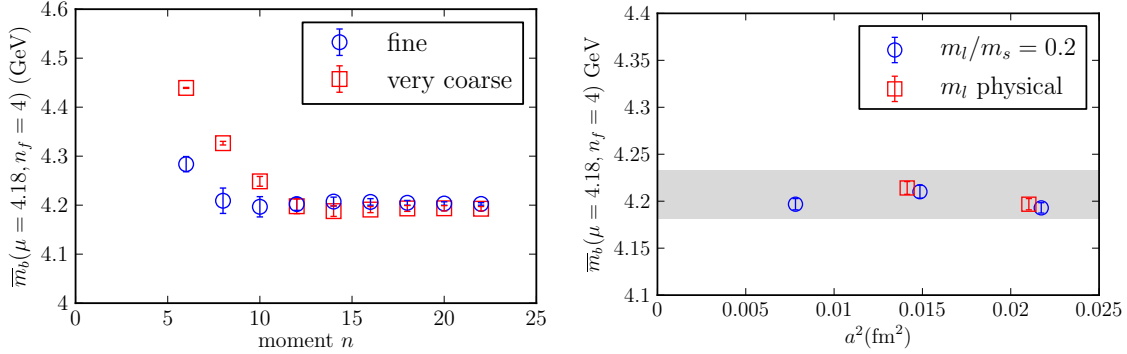


Figure 3: (Left)  $m_b^{\overline{\text{MS}}}$  extracted from the moments of NRQCD current-current correlators at two different lattice spacings from [11]. (Right) Results from the  $n = 18$  moment as a function of lattice spacing and for two different light-quark masses. The gray band gives the continuum determination with the total error budget.

They use simulation data consisting of ratios of meson masses,  $M_{hl}(m_h)/M_{hl}(m_h/\lambda)$ , computed for a series of masses  $m_h$  around the charm mass, e.g.:  $m_h^{(0)} = m_c$ ,  $m_h^{(1)} = \lambda m_c$ , ...,  $m_h^{(n)} = \lambda^n m_c$ . These ratios have the advantage that discretization effects proportional to  $(am_h)^2$  are largely canceled. From this data they construct the function

$$y(m_h, \lambda) = \lambda^{-1} \frac{M_{hl}(m_h)}{M_{hl}(m_h/\lambda)} \frac{\rho(m_h/\lambda)}{\rho(m_h)}. \quad (17)$$

The functions  $\rho(m_h)$  on the r.h.s. of Eq. (17) relate the pole mass to the  $\overline{\text{MS}}$  mass and are known to N<sup>3</sup>LO in perturbation theory.  $y(m_h, \lambda)$  satisfies  $\lim_{m_h \rightarrow \infty} y(m_h, \lambda) = 1$  on account of Eq. (16), and so its value can be interpolated between the charm region and the static limit using a motivated fit ansatz. Rewriting Eq. (17), the combination  $\lambda y(m_h, \lambda) \frac{\rho(m_h)}{\rho(m_h/\lambda)}$  is then a known function that evolves  $M_{hl}(m_h/\lambda)$  to  $M_{hl}(m_h)$ . Choosing  $\lambda$  such that  $M_{hl}(m_h^{(N)}) = M_{bl}^{\text{phys}}$  for some  $N$ , they determine the  $b$  mass from  $m_b = \lambda^N m_c$ .

## 5 Mass ratios

Mass parameters are inputs to lattice QCD simulations, these are pure numbers  $(am_0)$  corresponding to masses expressed in units of the lattice spacing  $a$ . There is one bare mass parameter for each quark in the simulation, and these must be tuned to reproduce the physics of QCD. The bare mass parameters are tuned by measuring low-energy observables such as meson masses, and requiring that these are equal to their physical values. After this set of observables has been used to tune the simulation parameters, one has a set of numbers  $\{(am_{ud0}), (am_{s0}), (am_{c0})\}$ . The



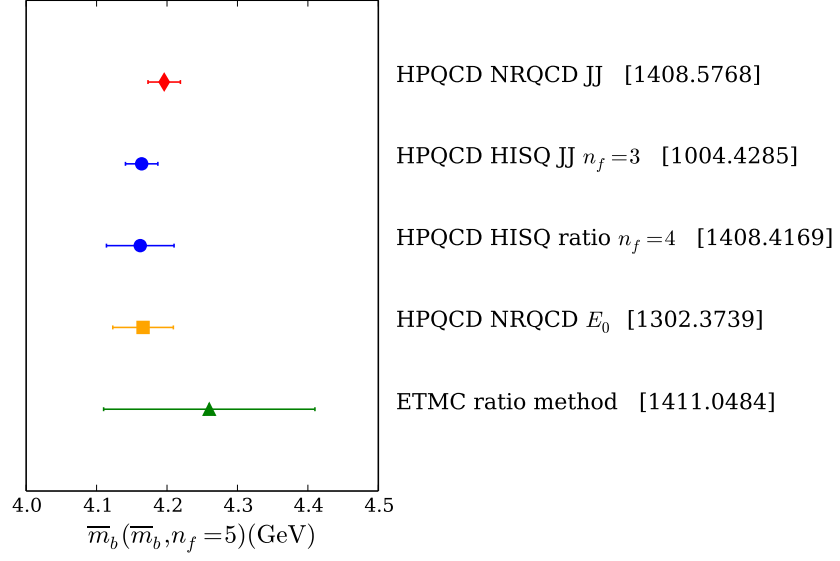


Figure 4: Comparison plot for determinations of  $m_b^{\overline{\text{MS}}}(m_b, n_f = 5)$ , computed from  $n_f = 2 + 1$  and  $n_f = 2 + 1 + 1$  simulations.

bare lattice inputs are defined at the cutoff scale and depend on the details of the discretization. However, ratios of input masses are equal to the ratios of  $\overline{\text{MS}}$  masses, up to discretization effects that vanish in the continuum,

$$\frac{am1_0}{am2_0} = \frac{m1^{\overline{\text{MS}}}(\mu)}{m2^{\overline{\text{MS}}}(\mu)} + \mathcal{O}(a^2). \quad (18)$$

Thus once the  $\overline{\text{MS}}$  mass is known for one quark in the theory, this can be converted to the  $\overline{\text{MS}}$  masses for the others using the input mass parameters.

An example of this is shown in Fig. 5 (left), for the input ratio  $m_{0c}/m_{0s}$  from [5]. In the continuum HPQCD find that

$$\frac{m_c(\mu, n_f)}{m_s(\mu, n_f)} = 11.652(65) \quad (19)$$

Using their result for  $m_c^{\overline{\text{MS}}}(\mu)$  from the current-current correlator method discussed in Sec. 3.1, they obtain

$$m_s^{\overline{\text{MS}}}(3 \text{ GeV}, n_f = 3) = 84.7(7) \text{ MeV}, \quad (20)$$

which is the most precise estimate to date. Fig. 5 (right) shows a result from [5] using input mass ratios to obtain  $m_b^{\overline{\text{MS}}}$ . Here the input mass is increased from  $m_{c0}$  towards

$m_{b0}$ , and finally an extrapolation performed to obtain

$$\frac{m_b(\mu, n_f)}{m_c(\mu, n_f)} = 4.528(54) \quad (21)$$

$$m_b^{\overline{\text{MS}}}(m_b, n_f = 5) = 4.162(48) \text{ GeV} \quad (22)$$

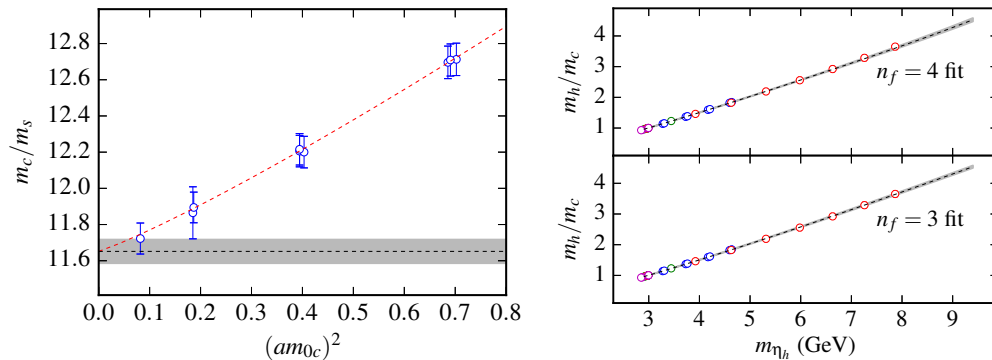


Figure 5: (Left) Continuum extrapolation of the bare quark mass ratio  $\frac{m_{0c}}{m_{0s}}$  from [5]. (Right) Extrapolation of  $\frac{m_{0h}}{m_{0c}}$  in  $m_{\eta_h}$  to  $m_{\eta_b}$  using simulation data from [5]. Magenta/green/blue/red points are from lattice spacings of 0.15/0.12/0.09/0.06 fm.

## 6 Conclusion

Recent progress in lattice determinations of charm and bottom quark mass was reviewed. In order to achieve (sub-)percent level uncertainties for these quantities, it is important that determinations come both from a variety of calculational strategies, and via independent measurements from different groups.

The most precise quoted values for  $c$  mass presently come from calculations of current-current correlators, comparing these to perturbation theory, where a heavy ( $\sim m_c$ ) input mass sets the scale  $\mu$ . The precision in the value of the charm mass can be cascaded to the other masses using bare quark-mass ratios, which are determined in the tuning of simulation parameters to their physical values.

Calculations of  $b$  mass are done either using an effective-theory framework for the  $b$  quark or extrapolating relativistic simulations from lower-mass region where discretization effects are under control. Extrapolation methods will continue to improve as ensembles with smaller lattice spacings become available. First steps have been taken towards a fully relativistic treatment of the  $b$  quark [5, 6]. This will lead not only to more precise values for the  $b$  itself, but through the use of mass ratios should improve determinations of the other quark masses as well.

## ACKNOWLEDGEMENTS

I would like to thank the organizers of Charm 2015 for a very enjoyable conference, and the participants for many illuminating discussions, in particular M. Padmanath, Sasa Prelovsek, and Vicent Mateu. I would like to thank Christine Davies, Yi-Bo Yang, Petros Dimopoulos, and Katsumasa Nakayama for providing material for this review, and Christine Davies for providing feedback on the manuscript.

## References

- [1] G. P. Lepage, P. B. Mackenzie and M. E. Peskin, arXiv:1404.0319 [hep-ph].
- [2] K. G. Chetyrkin, J. H. Kuhn and C. Sturm, Eur. Phys. J. C **48** (2006) 107 [hep-ph/0604234].
- [3] R. Boughezal, M. Czakon and T. Schutzmeier, Phys. Rev. D **74** (2006) 074006 [hep-ph/0605023].
- [4] A. Maier, P. Maierhofer, P. Marquard and A. V. Smirnov, Nucl. Phys. B **824** (2010) 1 [arXiv:0907.2117 [hep-ph]].
- [5] B. Chakraborty *et al.*, Phys. Rev. D **91** (2015) 5, 054508 [arXiv:1408.4169 [hep-lat]].
- [6] C. McNeile, C. T. H. Davies, E. Follana, K. Hornbostel and G. P. Lepage, Phys. Rev. D **82** (2010) 034512 [arXiv:1004.4285 [hep-lat]].
- [7] K. Nakayama, *et al.* [JLQCD Collaboration], Lattice 2015 conference [slides](#), to be published in PoS(LATT2015).
- [8] N. Carrasco *et al.* [European Twisted Mass Collaboration], Nucl. Phys. B **887** (2014) 19 [arXiv:1403.4504 [hep-lat]].
- [9] Y. B. Yang *et al.*, Phys. Rev. D **92** (2015) 3, 034517 [arXiv:1410.3343 [hep-lat]].
- [10] Z. Liu *et al.* [chiQCD Collaboration], Phys. Rev. D **90** (2014) 3, 034505 [arXiv:1312.7628 [hep-lat]].
- [11] B. Colquhoun, R. J. Dowdall, C. T. H. Davies, K. Hornbostel and G. P. Lepage, Phys. Rev. D **91** (2015) 7, 074514 [arXiv:1408.5768 [hep-lat]].
- [12] A. J. Lee *et al.* [HPQCD Collaboration], Phys. Rev. D **87** (2013) 7, 074018 [arXiv:1302.3739 [hep-lat]].
- [13] B. Blossier *et al.* [ETM Collaboration], JHEP **1004** (2010) 049 [arXiv:0909.3187 [hep-lat]].
- [14] A. Bussone *et al.*, arXiv:1411.0484 [hep-lat].